# Stoichiometry of Complex Formation between Copper(I) and the N-Terminal Domain of the Menkes Protein†

Paul A. Cobine,‡ Graham N. George,§ Donald J. Winzor,|| Mark D. Harrison,‡,⊥ Shadi Mogahaddas,‡,# and Charles T. Dameron*,‡

*National Research Center for Environmental Toxicology, University of Queensland, Coopers Plains, Queensland 4108, Australia, Stanford Synchrotron Radiation Laboratory, Stanford University, SLAC, P.O. Box 4393, Stanford, California 94309, and Department of Biochemistry, University of Queensland, Brisbane, Queensland 4072, Australia*

*Received January 4, 2000; Revised Manuscript Received March 14, 2000*

ABSTRACT: The inherent cellular toxicity of copper ions demands that their concentration be carefully controlled. The cellular location of the Menkes ATPase, a key element in the control of intracellular copper, is regulated by the intracellular copper concentration through the N-terminus of the enzyme, comprising 6 homologous subdomains or modules, each approximately 70 residues in length and containing a -Cys-X-X-Cys- motif. Based on the proposal that binding of copper to these modules regulates the Menkes ATPase cellular location by promoting changes in the tertiary structure of the enzyme, we have expressed the entire N-terminal domain (MNKr) and the second metal-binding module (MNKr2) of the Menkes protein in *E. coli* and purified them to homogeneity. Ultraviolet−visible, luminescence, and X-ray absorption spectroscopy show that copper and silver bind to the single module, MNKr2, with a stoichiometry of one metal ion per module. However, the array of six modules, MNKr, binds Cu(I) to produce a homogeneous conformer with 4 mol equiv of metal ion. The metal ions are bound in an environment that is shielded from solvent molecules. We suggest a model of the Menkes protein in which the Cu(I) binding induces tertiary changes in the organization of the six metal-binding domains.

Menkes disease is a genetic disorder characterized by a deficiency of serum copper and copper-dependent enzymes. This disorder is caused by mutations in the gene, *ATP7A* (GenBank Accession No. NM_000052), encoding the Menkes protein (*1*−*3*). The Menkes protein (MNK)[1] comprises 1500 amino acid residues and exhibits the characteristic elements of a P-type ATPase: a phosphorylation domain, an ATP-binding site, and a transmembrane ion channel. The P-type ATPases are a family of membrane proteins that form an aspartyl phosphate intermediate during transport of cations ($H^+$, $Na^+$, $K^+$, $Cu^+$, $Cd^{2+}$, $Hg^{2+}$) across the plasma membrane and other intracellular membranes (*4*). MNK shares significant sequence identity with other prokaryotic and eukaryotic P-type ATPases involved in membrane transport of copper, cadmium, mercury, and calcium (*5*−*8*).

High levels of MNK in the plasma membrane are associated with the resistance of cells to extracellular copper (*9*). *ATP7A* is not regulated at the transcription or translation levels. Instead, copper promotes the rapid translocation of MNK from its position in the trans-Golgi network to the plasma membrane (*10*). Plausibly, the MNK is helping protect the cells by exporting the excess copper. The amino-terminal domain of the Menkes protein, MNKr (residues 1−652), contains 6 conserved modules (MNKr1−6) comprising approximately 70 amino acid residues that are linked together by sequences that are predicted to be unstructured. Although the composition of these linking sequences is not conserved within the Menkes protein, the length of the tethers is conserved among the mammalian homologues. Each module contains a -Cys-X-X-Cys-binding motif (where X is any amino acid residue). Such -Cys-X-X-Cys- pairs are also found in metallothioneins, as well as in the yeast transcription factors ACE1 (*11*−*13*) and AMT1 (*14*), where the cysteinyl thiolates are involved in the binding of copper(I) ions in polymetallic clusters. In that regard, there is again no sequence conservation, apart from the -Cys-X-X-Cys- motif, between the MNKr modules and the metallothioneins or ACE1/AMT1. On the other hand, the conserved MNKr

† This investigation was supported by grants from the Australian Research Council. The Stanford Synchrotron Laboratory is funded by the Department of Energy, Office of Basic Energy Sciences. The Structural Molecular Biology program is supported by the National Institutes of Health Biomedical Research Technology Program, Division of Research Resources. Further support is provided by the Department of Energy, Office of Biological and Environmental Research.

* Address correspondence to this author at the National Research Center for Environmental Toxicology, University of Queensland, 39 Kessels Rd., Coopers Plains, Queensland 4108, Australia. (Phone) 61-7-3274-9009; (FAX) 61-7-3274-9003; (E-mail) c.dameron@mailbox.uq.edu.au.

‡ National Research Center for Environmental Toxicology, University of Queensland.

§ Stanford Synchrotron Radiation Laboratory, Stanford University.

|| Department of Biochemistry, University of Queensland.

⊥ Present address: Department of Biochemistry and Genetics, University of Newcastle, Newcastle-upon-Tyne, England, NE2 4HH.

# Present address: VAMC, Medical Research Department, Cleveland, OH 44106.

[1] Abbreviations: MNK, the 1500-residue protein deficient in patients with Menkes disease; MNKr, the amino-terminal regulatory domain of MNK (652 amino acids); MNKr2, the second amino-terminal subdomain of MNKr; MNKr4, the fourth amino-terminal subdomain of MNKr; XANES, X-ray absorption near-edge spectroscopy; EXAFS, extended X-ray absorption fine structure; UV−Vis, ultraviolet−visible spectroscopy.

10.1021/bi000015+ CCC: $19.00 
Published on Web 05/18/2000

modules are homologous with the metallochaperone MerP, which is involved in mercury transport (*15*), and CopZ (*16*) and Atx1 (*17*), which are involved in the transport of copper. These "copper chaperones" function as part of the mechanism for specific transport of copper ions to copper-dependent enzymes such as superoxide dismutase (*18*), cytochrome *c* oxidase (*19*), and FET3p (*17*). Indeed, the direct transfer of Cu(I) from the Cu(I)-chaperone CopZ to the Cu(I)-regulated repressor CopY has been demonstrated recently (*20*). Structural characterization of CopZ, Atx1, MerP, and the fourth module of the Menkes ATPase (MNKr4) shows that these proteins are very structurally similar (*21*). These modules are also found as metal-binding domains in multidomain metallochaperones, metal-ion reductases, and P-type ATPases for the metabolism of mercury, cadmium, and copper (*6*, *22*).

The current proposal is that copper regulates the location of the Menkes ATPase through tertiary structural changes induced by copper binding to the six tethered modules in the N-terminal domain. NMR analysis of the fourth module of the Menkes protein (MNKr4) confirms that each of the six subdomains or modules in MNKr consists of two α-helices and four antiparallel β-strands arranged in a $\beta^1$-$\alpha^1$-$\beta^2$-$\beta^3$-$\alpha^2$-$\beta^4$ global fold (*23*). Despite the flexibility of the metal-binding loop between α-helix 1 and β-sheet 2, Ag(I) binding causes very little perturbation in the tertiary structure of MNKr4 (*23*). More changes are induced when Cu(I) binds to the homologous metallochaperone CopZ (*24*). Induction or stabilization of distinct tertiary structures by metal binding is a hallmark of metalloregulatory proteins (*25*). The present UV−Vis, luminescence, and X-ray absorption spectroscopy studies show that, while an isolated module (MNKr2) binds Cu(I) with 1:1 stoichiometry (*26*), the array of six tethered modules in MNKr binds only 4 mol equiv of Cu(I). These results implicate Cu(I)-induced changes in the tertiary structure of the N-terminal domain of the Menkes ATPase that could be a regulatory element in the function of the enzyme.

## MATERIALS AND METHODS

*Preparation of Apo-proteins.* MNKr2 was purified, lyophilized, and subsequently dissolved in a minimal volume of 6 M guanidine hydrochloride−150 mM DTT−100 mM Tris/HCl, pH 7.9, for a 2 h reduction at 42 °C as described previously (*26*). The purification of MNKr followed our previous procedure (*27*) except for the addition of a dialysis step after resuspension of insoluble proteins in 6 M guanidine hydrochloride. After dialysis (6 h) against 50 mM Tris/HCl−200 mM NaCl−50 mM β-mercaptoethanol, pH 8.0, the insoluble fraction was removed by centrifugation. The soluble fraction was then resolved on Superdex 200 (Pharmacia) equilibrated with the same buffer, and the resulting pure MNKr was then treated as outlined for the production of apo-MNKr2. Anaerobic conditions were maintained throughout all subsequent procedures by conducting all steps in a LABCONCO Atmospure glovebox equipped with an oxygen scavenging system and maintained in a 95% $N_2$/5% $H_2$ atmosphere. All UV−visible and fluorescence spectra were carried out on samples sealed in screw-topped fluorescence cuvettes (Spectracell, Inc.) while in the anaerobic glovebox. To recover the reduced apoprotein, the solution was acidified to pH 2.0 and chromatographed on a Sephadex G-25 column equilibrated with 25 mM HCl. The fractions containing the protein were pooled and stored anaerobically at 4 °C. The reduction state of the protein was assessed by dithiodipyridine-quantification of thiols (*28*). These methods have been applied to the transcription factors ACE1 and AMT and the metallothioneins. In the case of these proteins and MNKr and MNKr2, the methods do lot lead to breakage of the peptide chain (data not shown). Moreover, circular dichroism studies of the second metal-binding domain of the Menkes protein have shown that this domain, homologous to the other five domains, has the same secondary structure whether purified with or without the use of denaturing conditions (*26*). This is entirely consistent with detailed studies of the homologous mercury-binding protein MerP (*29*). Secondary structure predictions on the sequences between the metal-binding domains in MNKr suggest they are not likely to adopt α-helical or β-sheet secondary structures. Furthermore, these sequences are not conserved between the various mammalian Menkes and Wilsons proteins, suggesting the specific sequences are not critical to the structure of the N-terminus. The length of the sequences is maintained but not the composition.

*Estimation of Protein Concentration.* Initially, the concentrations of MNKr and MNKr2 solutions were determined on the basis of quantitative amino acid analysis performed on a Beckman 6300 analyzer after hydrolysis in vacuo for 24 h at 110 °C in 6 M HCl supplemented with 0.01% phenol. Comparison of molar concentrations thus determined with the corresponding absorbances of the starting solutions yielded corrected molar absorptivities ($M^{-1}$ $cm^{-1}$) of 38 000 and 2500 for MNKr and MNKr2, respectively.

*Cu(I) Titration of MNKr2 and MNKr.* To determine the in vitro copper-binding stoichiometries of MNKr and MNKr2, aliquots of the purified apo-proteins were titrated with increasing molar equivalents of $[Cu(I)Cl]_x$ at fixed protein concentration (2 nmol in 1.5 mL) under anaerobic conditions. The reconstitutions were performed on samples with a reduction state >95% in accordance with the procedure described previously for metallothionein (*30*) and ACE1 (*11*). Briefly, the reduced protein was mixed at pH 2 with copper(I) and water, after which a concentrated buffer was added (with mixing) to adjust the pH to the desired level. Tris−chloride was used in the Cu(I) titrations of MNKr, whereas an imidazole−chloride buffer was used for the MNKr2 titrations. Cu(I) stock solution, stabilized as $[CuCl]_x^-$, was prepared by dissolving CuCl in 0.1 M HCl−1 M NaCl under anaerobic conditions in a LABCONCO anaerobic chamber. The titrations were monitored by absorption spectroscopy over the wavelength range 220−820 nm, although only the 220−420 nm range is shown. The broad range was used to ensure that Cu(II)−nitrogen-type complexes, which tend to absorb near 600 nm, were not being produced during the experiments. All spectra were recorded at 23 °C in anaerobically sealed screw-topped fluorescence cuvettes (Spectrocell) containing a total volume of 1.5 mL. After the spectral analysis, the copper concentration was verified by flame atomic absorption spectroscopy in a Varian A-875 series spectrometer.

*Spectroscopic Analyses.* Absorption spectra were recorded on a Cary U3 UV−Vis spectrophotometer. Luminescence spectra were recorded on a Perkin-Elmer LS 50B luminescence spectrometer with a 350 nm band-pass filter and

respective settings of 5 and 20 nm for the excitation and emission slits. Cuvettes were maintained at 23 °C in both instruments.

The Cu(I)−MNKr2 X-ray absorption spectroscopy (XAS) sample was prepared with an equimolar Cu(I):protein ratio and a final copper concentration of 0.9 mM, the metal:protein ratio being 0.95 for the corresponding analysis of an Ag(I)−MNKr2 sample. These samples were prepared in 100 mM sodium acetate buffer, pH 5.5, supplemented with 137 mM NaCl and 30% (v/v) glycerol. The Ag(I)−MNKr2 sample was lyophilized for transport to Stanford, where it was dissolved in degassed 40% glycerol/water (0.3 mL) immediately before flash-freezing of the sample. Cu(I)−MNKr samples were prepared anaerobically with a metal:protein ratio of 4 and a final copper concentration of 0.8 mM in 100 mM Tris/HCl, pH 7.9, containing 100 mM NaCl, 0.01% (v/v) NP-40 (Sigma), and 40% (v/v) glycerol. The protein's stoichiometry did not change during ultrafiltration; the recovery of protein was greater than 80%. Ultrafiltration of 6- and 8Cu(I) preparations has led to a reduction in stoichiometry of the preparations (*27*, *31*), suggesting a stoichiometry of 4Cu(I) per protein is preferred. No excess of reducing agent was added to these samples during preparation because of possible consequent interference in data collection and interpretation. Although chloride can potentially complicate EXAFS data analysis, no special attempts were made to exclude chloride ions, which can be an important effector of the binding of Cu(I) to Cu(I)−proteins (*32*).

Copper and silver K-edge X-ray absorption spectroscopic data were collected at the Stanford Synchrotron Radiation Laboratory (SSRL) with the SPEAR storage ring containing 50−100 mA at 3.0 GeV. The unfocused wiggler beam line 7-3 was used with the wiggler operating at a field of 1.8 T. A Si(220) double-crystal monochromator was used with an upstream vertical aperture of 1 mm, and harmonic rejection was accomplished by detuning one monochromator crystal to approximately 50% off-peak. The incident X-ray intensity was monitored using an argon-filled (for silver) or nitrogen-filled (for copper) ionization chamber, and X-ray absorption was measured as the X-ray Kα fluorescence excitation spectrum with an array of 13 germanium detectors (*33*). Samples were maintained at a temperature of approximately 10 K during data collection using a liquid helium flow cryostat. Eighteen 20-min scans were accumulated, and the absorption of metal foil standards was measured simultaneously by transmittance. The energy scale was calibrated with reference to the lowest energy inflection point of the foil, which was assumed to be 8980.3 and 25515 eV for copper and silver, respectively.

Quantitative analysis of the extended X-ray absorption fine structure (EXAFS) oscillations, $\chi(k)$, entailed curve-fitting with the EXAFSPAK suite of computer programs (http://ssrl.slac.stanford.edu/exafspak.htm) on the basis of ab initio theoretical phase and amplitude functions calculated with the program FEFF V7.02 (*34*, *35*). No smoothing, Fourier-filtering, or related manipulation was performed upon the data. Respective values for the threshold energy (i.e., energy zero for $k$) were taken as 9000.0 and 25525.0 eV for Cu K-edge and Ag K-edge data, respectively.

*Sedimentation Equilibrium Studies*. The molecular masses of MNKr and its complex with copper in Tris−chloride buffer, pH 7.9, were measured by sedimentation equilibrium in order to ascertain whether the binding of metal ion led to aggregation of the protein. A Beckman XL-I ultracentrifuge operated at 9000 rpm and 20 °C was used for these experiments. Because of the susceptibility of the MNKr sulfhydryl groups to oxidation, the centrifuge cells were assembled and filled anaerobically in a glovebox.

Spectrophotometric records at 230 nm of the resulting sedimentation equilibrium distributions were analyzed in accordance with the expression:

$$A_{230}(r) = A_{230}(0)\exp[M_A(1 - \upsilon_A\rho_s)\omega^2 r^2/(2RT)] \quad (1)$$

in which $A_{230}(r)$ is the absorbance at radial distance $r$ in an experiment conducted at angular velocity $\omega$ and absolute temperature $T$ in a buffer with density $\rho_s$ and $R$ is the universal gas constant. $A_{230}(0)$ denotes the absorbance at the reference radial position, taken as the center of rotation ® = 0). Nonlinear regression analysis of the radial dependence of $A_{230}$ in terms of eq 1 was used to obtain two curve-fitting parameters—the notional absorbance at the center of rotation, and the buoyant molecular mass, $M_A(1 - v_A\rho_s)$. To effect the conversion of the latter parameter to a molecular mass ($M_A$) the partial specific volume ($\upsilon_A$) of MNKr has been taken as 0.740 mL/g, deduced from the amino acid composition (*36*), whereas the buffer density of 1.0066 g/mL was determined at 20 °C by standard procedures in an Anton−Paar density meter.

## RESULTS

The efficiency of the purifications of the Menkes domains was increased when they were isolated in their apo state because the heterogeneity of the metalated proteins caused some loss of material during the purification. Care was taken during the purification and subsequent treatments to avoid contamination with spurious metals. These purification methods were chosen to avoid the use of fusions that might interfere with the folding, metal-binding, or spectroscopic analyses of the proteins. Although these methods made the purifications slightly more difficult, it enabled experiments to be conducted at higher concentrations of MNKr than those performed on the Menkes and Wilson proteins as maltose-binding protein or GST fusions, presumably the fusions were limiting the solubility (*37*, *38*).

*Titration of MNKr with Cu(I)*. Titration of the six tethered modules of MNKr with copper is summarized in Figure 1A, which illustrates the formation of charge-transfer bands near 250 nm. On the basis that the increase in absorbance at 254 nm becomes Cu(I)-independent after the addition of 4 mol equiv of metal ion (Figure 1B), MNKr exhibits a stoichiometry of 4 toward Cu(I). Titrations performed in the presence of excess reductants (glutathione and cysteine) failed to increase the stoichiometry (data not shown).

Seclusion of Cu(I)−thiolates, either individually or in clusters of metal ions, leads to the formation of Cu(I)−thiol-specific luminescence at room temperature (*39*). Fluorescence scans of Cu(I)−MNKr solutions exhibit an emission band at 600 nm (Figure 1C), which is similar to those seen in ACE and MT (*11*−*14*). Under the same conditions, no luminescence is observed for a mixture of Cu(I) and the single module of MNKr2 (− · −, Figure 1C). For MNKr, the increase in luminescence at 600 nm increases with

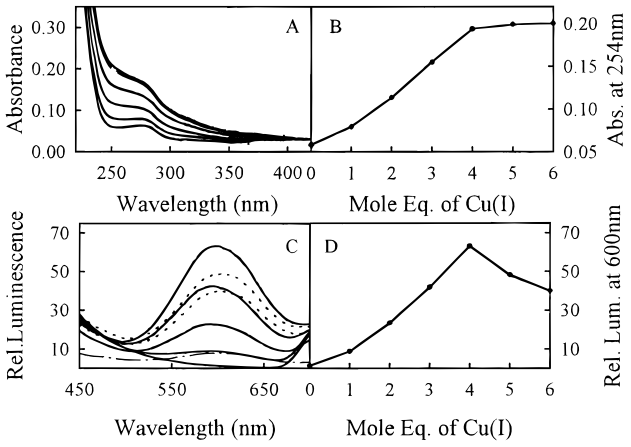


FIGURE 1: Spectral analysis of the stoichiometry of the interaction between Cu(I) and a fixed amount (2 nmol in 1.5 mL of Tris−chloride, pH 7.9) of MNKr. (A) Effect of increasing Cu:protein molar ratio on the UV−Vis spectrum (220−420 nm). (B) Dependence of $A_{254}$ upon the copper:protein molar ratio. (C) Corresponding effect of Cu(I) on the luminescence at molar metal:protein ratios below (0:1, 1:1, 2:1, 3:1) (—) and above (5:1, 6:1) (− − −) the end-point value of 4; (− · −) corresponding spectrum for the 1:1 Cu−MNKr2 complex. (D) Dependence of the relative luminescence at 600 nm upon the Cu:protein molar ratio.

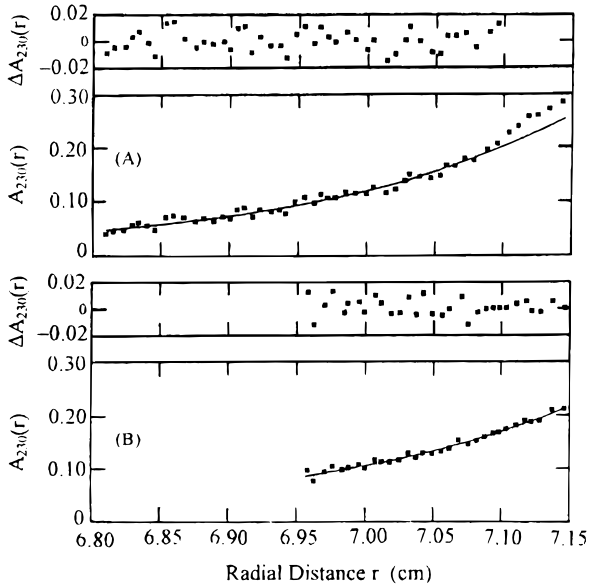


FIGURE 2: Sedimentation equilibrium distributions (■) at 9000 rpm and 20 °C for (A) apo-MNKr and (B) its saturated copper complex in Tris−chloride, pH 7.9. Solid lines are the best-fit descriptions of the data in terms of eq 1, the degree of goodness-of-fit to such description being shown in the upper panel by the radial dependence of the difference between the experimental and calculated absorbances at 230 nm ($\Delta A_{230}$).

copper:protein ratio to a maximum of 4 Cu(I) ions per protein molecule (Figure 1D), a result consistent with the 4:1 stoichiometry deduced from the UV−Vis spectroscopy data (Figure 1B). Copper-to-protein ratios greater than 4 led to a red shift of 5 nm and a decrease in emission intensity caused by an increase in the exposure of the Cu(I) cluster to solvent by the incorporation of excess copper (*11*, *39*). The addition of copper in excess of that sheltered from the solvent has been associated with the formation of unstable clusters in the metallothioneins (*39*) and a decrease in the activity of transcription factor AMT1 (*14*). Similarly, the decrease in luminescence observed for MNKr at stoichiometries above 4Cu(I) per protein indicates that the metal-binding sites have been perturbed. This perturbation may allow these metal ions to be more easily removed.

The specific incorporation of four Cu(I) ions into a solvent-shielded (luminescent) environment in MNKr, which has six putative copper-binding sites, suggests that the protein may contain individual shielded metal-binding sites or clusters analogous to those found in Cu(I)−MT (*39*) and the Cu(I)-regulated transcription factors ACE1 (*11*) and AMT1 (*14*). To ensure that the metals were held intramolecularly, in a single N-terminal MNKr molecule, rather than intermolecularly, between multiple molecules or an aggregate of molecules, the oligomeric state was investigated by sedimentation equilibrium (Figure 2).

*Effect of Cu(I) on the Macromolecular State of MNKr*. Interpretation of results for the titration of MNKr with Cu(I) ion is clearly conditional upon establishing the effect of metal ion upon the macromolecular state of the protein in the environment to be used for the titration. Figure 2A presents a sedimentation equilibrium distribution (■) for MNKr in the Tris−chloride buffer (pH 7.9), together with the best-fit description (—) in terms of eq 1. The resultant molecular mass (±2 SD) of 77 000 (±5000) Da is in reasonable accord with the value of 74 200 Da that is calculated from the amino acid composition. The slight but significant departure from this best-fit description in the vicinity of the cell base signifies the presence of a small amount (<5%) of aggregated MNKr, presumably reflecting persistent trace amounts of oxygen in the sample subjected to sedimentation equilibrium. No such evidence of heterogeneity is found for the MNKr complex with copper (Figure 2B). Furthermore, the molecular mass of 74000 (±5000) Da that is obtained from this sedimentation equilibrium distribution signifies that the interactions of Cu(I) with MNKr must be explained in intramolecular terms because of the failure of metal binding to effect association of the protein monomer.

We have observed previously (*27*) that MNKr can accept 8 Cu(I) ions; this complex is readily converted to a more stable form with 4:1 stoichiometry by concentration of the protein solution or by gently heating it to 37 °C and allowing it to cool to 23 °C. Generation of the 4:1 species by concentration of a Cu(I)−MNKr complex with 6:1 stoichiometry has also been reported by Ralle et al. (*31*).

*X-ray Absorption Studies*. A more detailed description of the metal binding in the 1:1 Cu(I)−MNKr2 and Ag(I)MNKr2 species as well as in the 4:1 Cu(I)−MNKr complex has been obtained by X-ray absorption spectroscopy.

Cu K-edge X-ray absorption near-edge spectra (XANES) of the three complexes are shown in Figure 3 together with those for Cu(I) model compounds (Figure 3A). The copper−protein spectra for the MNKr2 and MNKr complexes (Figure 3B) show no 1s to 3d transition near 8980 eV (1 eV = 1.6022 × $10^{-19}$ J)—a finding that confirms the cuprous oxidation state of the copper−protein complexes. The peak at approximately 8983 eV has been considered to indicate the presence of digonally coordinated Cu(I) (*13*, *40*). From the spectra for model compounds (Figure 3A), the intensity of this peak is greatest for the digonally coordinated complex and least intense for the purely trigonal complex. As discussed previously (*13*), the quantitative estimation of the fraction of digonal copper is difficult for proteins with

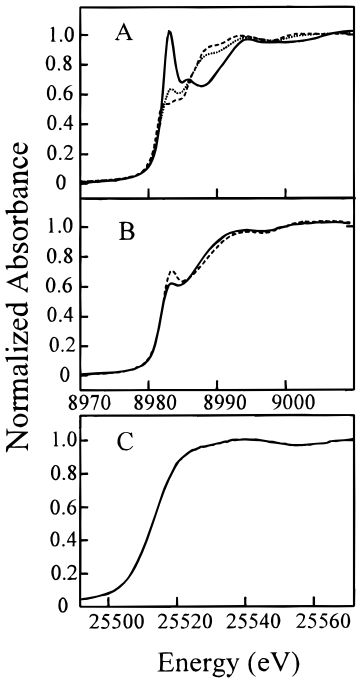


FIGURE 3: X-ray absorption near-edge spectra for metal complexes of MNKr and MNKr2. (A) Copper K-edge near-edge spectra for three cuprous−thiolate model complexes with different fractions of digonal copper: (− − −) $(Me_4N)_2[Cu_4(SPh)_6]$ (0% digonal); (•••) $(Et_4N)[Cu_5(SBut)_6]$ (60% digonal); (—) $[N(C_3H_7)_4]$-$Cu(SC_{10}H_{12})_2$ (100% digonal) (*46*). (B) Copper K-edge near-edge spectra for Cu(I)MNKr2 (—) and $[Cu(I)]_4$MNKr (− − −). (C) Silver K-edge near-edge spectrum of MNKr2 reconstituted with 0.95 mol equiv of Ag(I).

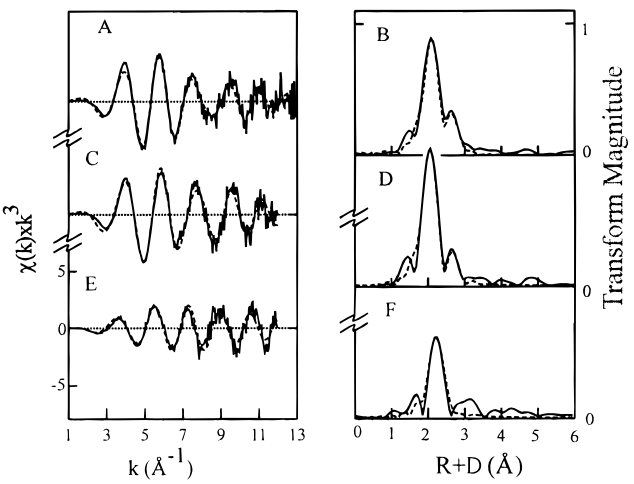


FIGURE 4: K-edge EXAFS (left-hand panel) and Fouier transforms (right-hand panel) for metal−ion complexes with MNKr2 and MNKr. The solid line shows the experimental data and the broken line the best fits. The Cu K-edge Fourier transforms and EXAFS have been phase-corrected for metal−sulfur backscattering. Panels A and C show, respectively, the EXAFS of 1Cu(I)−MNKr2 and 4Cu(I)−MNKr. The corresponding transforms are show in panels B and D. The silver K-edge EXAFS for 1Ag(I)−MNKr2 is shown in panel E and the respective transform in panel F.

multiple sites for copper, but the intensity of this feature in the spectra is certainly suggestive of a high fraction of digonally coordinated copper in the complexes with MNKr2 and MNKr (Figure 3B). The Ag K-shell X-ray absorption near-edge spectrum of MNKr2 is shown in Figure 3C, where the lack of features reflects the very large line widths resulting from the short core-hole lifetimes at the Ag K-edge X-ray energy. Further evidence on the coordination status of the metal ion is sought from the Cu−S and Ag−S bond lengths determined from EXAFS curve-fitting analysis.

The copper and silver K-edge EXAFS, best-fits, and associated Fourier transforms for MNKr2 are shown in Figure 4, the parameters derived from the curve-fitting analysis being summarized in Table 1. The copper EXAFS are dominated by the Cu−S backscattering but coupled with smaller outer features due to Cu−Cu backscattering. The inclusion of lighter scatterers such as O and N did not improve the fit. Curve-fitting analysis implicates between two and three Cu−S interactions with a mean Cu−S distance of 2.240 Å for MNKr2 (Figure 4A) and 2.207 Å for MNKr (Figure 4B); the rather large Debye−Waller factors suggest some static disorder in the samples.

As discussed by Pickering et al. (*13*), the best-fit Cu−S coordination number of 3 is subject to rather poor accuracy because of a high mutual correlation with the Debye−Waller factor. This contrasts with the excellent accuracy of EXAFS-derived bond lengths. Cuprous−thiolate complexes with digonally coordinated copper typically exhibit Cu−S bond lengths of about 2.16 Å, while those in trigonal copper coordination exhibit Cu−S bond lengths of about 2.28 Å. Consequently, EXAFS suggest that some of the coppers present in the MNKr sample, and perhaps the MNKr2 sample, are digonally coordinated. Application of the method outlined by Pickering et al. (*13*) yields an estimate of about 72% for the fraction of digonally coordinated Cu(I) in the MNKr sample. This contrasts with other cuprous−thiolate proteins, for which the fraction of digonal copper is generally very low.

The Cu−Cu EXAFS also show a large Debye−Waller factor, indicating the existence of some variability in Cu−Cu distances about the mean value *R* (Table 1) within the resolution of the data (∼0.15 Å). The observation that the Cu−Cu distance of approximately 2.6 Å is shorter than that found in cuprous−thiolate cluster proteins such as metallothionein (*13*) is consistent with the shorter Cu−S bond length observed in MNKr.

The silver K-edge EXAFS and transform of Ag(I)−MNKr2 are shown in Figure 4C, together with the Fourier transform and best-fit. The EXAFS is dominated by Ag−S interactions, and inclusion of light scatterers such as Ag−O and Ag−N again did not improve the fit. A Ag−Ag scatter was not observed. Comparison of the estimated Ag−S bond length of 2.39 Å (Table 1) with average bond lengths of 2.38 and 2.55 Å for two-coordinate and three-coordinate Ag−S complexes (Cambridge Crystallographic Data Base) strongly supports the presence of a digonally coordinated metal ion in the 1:1 Ag−MNKr2 complex.

## DISCUSSION

The regulation of Menkes protein location depends on the copper-binding properties of the N-terminal domains (*10*). Individually, the second domain of the Menkes protein (MNKr2) maximally binds 1 mol equiv of copper(I) (*26*) while MNKr binds 4 mol equiv of Cu(I). MNKr2 binds Cu(I) in a site that is poorly shielded from the surrounding solvent as evidenced by the lack of Cu−thiolate specific luminescence (Figure 1C). The XANES data (Figure 3) and the Cu−S bond length (Figure 4 and Table 1) of MNKr2

Table 1: Parameters Calculated from Unrestricted Curve Fitting of Reconstituted Cu(I)−MNKr2, Ag(I)−MNKr2, and 4Cu(I)−MNKr

| | | M−S | | | M−M | | | | |
|---|---|---|---|---|---|---|---|---|---|
| protein | Me | $N^a$ | $R$ (Å) | $\sigma^2$ (Å$^2$) | $N$ | $R$ (Å) | $\sigma^2$ (Å$^2$) | $\Delta E_o$ (eV) | error$^b$ |
| MNKr2 | Cu | 3 | 2.240(5)$^c$ | 0.0098(3) | 1 | 2.638(7) | 0.0101(6) | −17.5(8) | 0.354 |
| MNKr2 | Ag | 2 | 2.381(6) | 0.0048(3) | – | – | – | −14.6(16) | 0.523 |
| MNKr | Cu | 3 | 2.207(5) | 0.0088(3) | 0.5 | 2.631(7) | 0.0065(7) | −19.1(9) | 0.372 |

[a] EXAFS curve fitting yields values for the mean coordination number per Cu/Ag ($N$ for M−S and $N$ for M−M interactions), the mean interatomic distance ($R$), and the mean-square deviation in $R$ ($\sigma^2$), the Debye−Waller factor. For the Cu K-edge data, the coordination numbers were determined to be between 2 and 3. The values given are for $N = 3$, but an almost identical fit could be obtained with $N = 2$. [b] The fit error is defined as $\Sigma k^6(\chi_{exptl} - \chi_{calcd})^2/\Sigma k^6\chi_{exptl}^2$. [c] The values in parentheses are the estimated standard deviations obtained from the diagonal elements of the covariance matrix. We note that these precisions and accuracies are expected to be somewhat higher (typically ±0.02 Å for $R$, and ±25% for $N$ and $\sigma^2$).

implicate a mixture of digonally, approximately 70%, and trigonally coordinated Cu(I). Similar data have been obtained for the copper chaperone Atx1 (*41*). For a two-coordinate molecule, the cysteine sulfurs of the individual modules would suffice; but for a three-coordinate species, it is plausible that a portion of the third ligands could come from a bridging thiolate contributed by an adjacent MNKr2 or another module in MNKr. Although the Atx1 data were collected in the absence of chloride, this sample had a copper(I) to protein ratio of 0.7, leading to the possibility that the thiols from the apo-protein could have complicated the data, and may have had some additional low molecular weight thiols. Coincident with the small portion of trigonally bound copper(I), there is also some indication of Cu−Cu scatter in MNKr2 (Figure 4 and Table 1). This Cu−Cu interaction may be the result of the Cu(I) ions being ligated by shared intermolecular thiolates. Shared ligands are common among the Cu(I)-binding proteins such as the MT and AMT1. There was no metal to metal scatter observed in the Ag(I)−MNKr2 sample, possibly due to the preference of Ag(I) for 2-coordinate ligation.

The spectrophotometric titrations in conjunction with analytical centrifugation demonstrate that the interaction of Cu(I) with MNKr leads to stabilization of a 75 KDa monomer containing 4 Cu(I) ions in a solvent-shielded environment (Figures 1 and 3). EXAFS suggests that MNKr binds the Cu(I) with strong digonal character, approximately 70%, as did MNKr2. The observation of Cu−Cu scatter peaks in MNKr (Figure 4) would be consistent with the existence of some intermodular as well as intramodular copper, particularly in light that intermolecular Cu bridges are precluded by the sedimentation equilibrium data (Figure 2). Intramolecular copper bridging thiolates have been found in metallothioneins (*42*) and ACE1 (*11*), both of which form luminescent Cu(I):S cores. Plausibly, the tethering of six individual copper(I)−chaperone-like modules links them into an array that promotes interactions between the modules in vitro and limits the number of bound Cu(I) ions to 4. There has been an earlier report of Cu:protein stoichiometries of 6.5−7.3 for a glutathione transferase fusion with the N-terminus of the homologous Wilson protein (*38*), a finding which suggests that the protein can bind Cu(I) in excess of the predicted six metal ions. Indeed, we have reported the existence of an 8Cu(I)−MNKr complex that lost Cu(I) during ultrafiltration to become a 4Cu(I)−MNKr complex (*27*). The in vitro studies performed by Lutsenko et al. (*37*) with maltose-binding protein fusion of the N-termini of Menkes and Wilson proteins also signify a range of possible Cu(I):protein stoichiometries: 3.0−6.5 for Wilson protein and 3.7−5.5 for Menkes protein. Based on the direct purification of the fusion complex, it was concluded (*37*) that the Wilson protein bound 5.75 (±0.15) Cu(I) ions, the corresponding value for the Menkes protein being 5.39 (±0.26) Cu(I) ions. Inasmuch as the stoichiometry for the latter preparation is decreased to 4 by concentration of the sample (*31*), the finding may well reflect the average copper content of a mixture of conformers prior to attainment of the final equilibrium state. Certainly it is possible that the Cu:protein stoichiometries observed here and by others (*37*, *38*) may be artifactual since in vivo the modules in the intact Menkes protein and the related Wilson protein may not accumulate copper but instead may pass the metals directly to the ATPase domain. Nevertheless, it is clear from recent in vivo studies that copper binding to the amino terminus does play a crucial regulatory role (*43*, *44*). Although the ATPase does not require the domains for metal transport activity, it does require them for copper sensing and/or relocation to the plasma membrane. Relocation to the plasma membrane is required for detoxification, which remains the main focus of Menkes research activity. Since these studies suggest that only a single domain is needed, it is unclear why the protein has an additional five domains. Presuming the copper-induced trafficking is reliant on an induced conformational change as proposed, then the additional domains may increase the sensitivity of the reaction through its enhanced conformational change. In view of the present findings, we propose a model for the metalloregulation of MNK in which the Cu(I)-induced conformational changes in the structure of the modules and also of the modular array lead the relocation of the Menkes protein to the plasma membrane. To that end, NMR studies (*15*) have shown that Hg stabilizes the -Cys-X-X-Cys- loop and promotes a change in the α-helices in the mercury scavenger MerP, a homologue of MNKr2, and the other five modules in MNKr. Indeed, similar changes have been reported for the fourth domain of the Menkes protein (*23*) and for the copper chaperone CopZ (*24*).

Rearrangements at the module level alone do not suffice to account for the present fluorescence and EXAFS data. Specifically, the observation of Cu(I)-specific luminescence for the complete array of modules (MNKr) signifies protection of the copper ion from solvent exposure—a finding consistent with the creation of a hydrophobic environment by reorganization of the whole modular array to allow intermodular as well as intramodular copper interactions. The consequent hydrophobic shielding of Cu(I) from the aqueous environment may avert copper-induced oxidative damage in the cell during activation of the Menkes protein. The EXAFS results for the whole modular array (MNKr) are best fit with three Cu−S linkages of similar lengths, but the large Debye−Waller factor does suggest some static disorder in the bond

lengths. It is possible that a ligand was contributed by $Cl^-$, although the bond length is somewhat long and this would not explain the Cu−Cu scatter peak. Although chloride does not compete well for Cu(I) against thiolates in aqueous systems, in particular we have observed that $Cl^-$ has no tendency to extract Cu(I) from MNKr2 or MNKr. The exact nature of the Cu(I) binding in the Menkes ATPase and demonstration of a Cu(I) core as found in MT, ACE1, AMT1, and Mac will require additional EXAFS studies with and without anions.

## ACKNOWLEDGMENT

We gratefully acknowledge receipt of the amino-terminal portion of the Menkes gene from Julian F. B. Mercer in the form of the pQE30-53/4 plasmid. We are indebted to Martin J. George of SSRL for use of his data collection software and to Ingrid J. Pickering for assistance with the data collection there. The skilled technical assistance of Lyle E. Carrington in the conduct of the ultracentrifugation experiments is also gratefully acknowledged. We thank James Penner-Hahn of the University of Michigan for generously allowing us access to XAS data on the 100% digonal cuprous−thiolate complex shown in Figure 3.

## REFERENCES

1. Mercer, J. F., Livingston, J., Hall, B., Paynter, J. A., Begy, C., Chandrasekharappa, S., Lockhart, P., Grimes, A., Bhave, M., and Siemieniak, D. (1993) *Nat. Genet. 3*, 20−25.
2. Chelly, J., Tumer, Z., Tonnesen, T., Petterson, A., Ishikawa-Brush, Y., Tommerup, N., Horn, N., and Monaco, A. P. (1993) *Nat. Genet. 3*, 14−19.
3. Vulpe, C., Levinson, B., Whitney, S., Packman, S., and Gitschier, J. (1993) *Nat. Genet. 3*, 7−13.
4. Penderson, P., and Carafoli, E. (1987) *Trends Biochem. Sci. 12*, 146−150.
5. Silver, S., Nucifora, G., Chu, L., and Misra, T. (1989) *Trends Biochem. Sci. 14*, 16−20.
6. Silver, S., and Ji, G. (1994) *Environ. Health Perspect. 102, Suppl. 3*, 107−113.
7. Solioz, M. (1996) in *Ion Pumps* (Andersen, J. P., Ed.) JAI Press, London.
8. Bull, P. C., Thomas, G. R., Rommens, J. M., Forbes, J. R., and Cox, D. W. (1993) *Nat. Genet. 5*, 327−337.
9. Camakaris, J., Petris, M. J., Bailey, L., Shen, P., Lockhart, P., Glover, T. W., Barcroft, C. L., Patton, J., and Mercer, J. F. B. (1995) *Hum. Mol. Genet. 4*, 2117−2123.
10. Petris, M. J., Mercer, J. F. B., Culvenor, J. G., Lockhart, P., Gleeson, P. A., and Camakaris, J. (1996) *EMBO J. 15*, 6084−6095.
11. Dameron, C. T., Winge, D. R., George, G. N., Sansone, M., Hu, S., and Hamer, D. (1991) *Proc. Natl. Acad. Sci. U.S.A. 88*, 6127−6131.
12. Winge, D. R., Dameron, C. T., George, G. N., Pickering, I. J., and Dance, I. G. (1993) in *Bioinorganic Chemistry of Copper* (Karlin, K. D., and Tyeklar, Z., Eds.) pp 110−123, Chapman & Hall, New York.
13. Pickering, I. J., George, G. N., Dameron, C. T., Kurtz, B., Winge, D. R., and Dance, I. G. (1993) *J. Am. Chem. Soc. 115*, 9498−9505.
14. Thorvaldsen, J. L., Sewell, A. K., Tanner, A. M., Peltier, J. M., Pickering, I. J., George, G. N., and Winge, D. R. (1994) *Biochemistry 33*, 9566−9577.
15. Steele, R. A., and Opella, S. J. (1997) *Biochemistry 36*, 6885−6895.
16. Odermatt, A., and Solioz, M. (1995) *J. Biol. Chem. 270*, 4349−4354.
17. Lin, S.-J., Pufahl, R. A., Dancis, A., O'Halloran, T. V., and Culotta, V. C. (1997) *J. Biol. Chem. 272*, 9215−9220.
18. Culotta, V. C., Klomp, L. W. J., Strain, J., Casareno, R. L. B., Krems, B., and Gitlin, J. D. (1997) *J. Biol. Chem. 272*, 23469−23472.
19. Glerum, D. M., Shtanko, A., and Tzagoloff, A. (1996) *J. Biol. Chem. 271*, 14504−14509.
20. Cobine, P., Wickramasinghe, W. A., Harrison, M. D., Weber, T., Solioz, M., and Dameron, C. T. (1999) *FEBS Lett. 445*, 27−30.
21. Harrison, M. D., Jones, C. E., and Dameron, C. T. (1999) *J. Biol. Inorg. Chem. 4*, 145−153.
22. Solioz, M., Odermatt, A., and Krapf, R. (1994) *FEBS Lett. 346*, 44−47.
23. Gitschier, J., Moffat, B., Reilly, D., Wood, W. I., and Fairbrother, W. J. (1998) *Nat. Struct. Biol. 5*, 47−54.
24. Wimmer, R., Herrmann, T., Solioz, M., and Wuthrich, K. (1999) *J. Biol. Chem. 99*, 22597−22603.
25. O'Halloran, T. V. (1993) *Science 261*, 715−725.
26. Harrison, M. D., Meier, S., and Dameron, C. T. (1999) *Biochim. Biophys. Acta 1453*, 254−260.
27. Cobine, P., Harrison, M. D., and Dameron, C. T. (1999) *Adv. Exp. Med. Biol. 448*, 153−164.
28. Grassetti, D. R., and Murray, J. F., Jr. (1967) *Arch. Biochem. Biophys. 119*, 41−49.
29. Aronsson, G., Brorsson, A.-C., Sahlman, L., and Jonsson, B.-H. (1997) *FEBS Lett. 411*, 359−364.
30. Byrd, J., Berger, J. M., McMillin, D. R., Wright, C. F., Hamer, D., and Winge, D. R. (1988) *J. Biol. Chem. 263* (14), 6688−6694.
31. Ralle, M., Cooper, M. J., Lutsenko, S., and Blackburn, N. J. (1998) *J. Am. Chem. Soc. 120*, 13525−13526.
32. Davis-Kaplan, S., Askwith, C. C., Bengtzen, A. C., Radisky, D., and Kaplan, J. (1998) *Proc. Natl. Acad. Sci. U.S.A. 95*, 13641−13645.
33. Cramer, S. P., Tench, O., Yocum, M., and George, G. N. (1988) *Nucl. Instrum. Methods Phys. Res. 266*, 586−591.
34. Rehr, J. J., Mustre de Leon, J., Zabinsky, S. I., and Albers, R. C. (1991) *J. Am. Chem. Soc. 113*, 5135−5140.
35. Mustre de Leon, J., Rehr, J. J., and Zabinsky, S. I. (1991) *Phys. Rev. B: Condens. Matter Mater. Phys. 44*, 4146−4156.
36. Laue, T. M., Shah, B. D., Ridgeway, T. M., and Pelletier, S. L. (1992) in *Analytical Ultracentrifugation in Biochemistry and Polymer Science* (Harding, S. E., Rowe, A. J., and Horton, J. C., Eds.) pp 90−125, Royal Society of Chemistry, Cambridge, U.K.
37. Lutsenko, S., Petrukhin, K., Cooper, M. J., Gilliam, C. T., and Kaplan, J. H. (1997) *J. Biol. Chem. 272*, 18939−18944.
38. DiDonato, M., Narindrasorasaki, S., Forbes, J. R., Cox, D. W., and Sarkar, B. (1997) *J. Biol. Chem. 272*, 33279−33282.
39. Stillman, M. J., and Gasyna, Z. (1991) *Methods Enzymol. 205*, 540−555.
40. Kau, L., Spira-Solomon, D. J., Penner-Hann, J. E., Hodgson, K. O., and Solomon, E. I. (1987) *J. Am. Chem. Soc. 109*, 6433−6442.
41. Pufahl, R. A., Singer, C. P., Peariso, K. L., Lin, S.-J., Schmidt, P. J., Fahrni, C. J., Culotta, V. C., Penner-Hahn, J. E., and O'Halloran, T. V. (1997) *Science 278*, 853−856.
42. Robbins, A. H., and Stout, C. D. (1992) in *Metallothioneins: synthesis, structure and properties of metallothioneins, phytochelatins and metal thiolate complexes* (Stillman, M. J., Shaw, C. F., and Suzuki, K. T., Eds.) Chapter 3, pp 31−54, VCH Publishers, Inc., New York.
43. Strausak, D., La Fontaine, S., Hill, J., Firth, S. D., Lockhart, P. J., and Mercer, J. F. B. (1999) *J. Biol. Chem. 274*, 11170−11177.
44. Voskoboinik, I., Strausak, D., Greenough, M., Brooks, H., Petris, M., Smith, S., Mercer, J. F. B., and Camakaris, J. (1999) *J. Biol. Chem. 274*, 22008−22012.

BI000015+